Egypt. J. Chem. **Vol. 67**, No. 5 pp.685 – 693 (2024)

Egyptian Journal of Chemistry

http://ejchem.journals.ekb.eg/

Electrochemical and Mechanical Characterization of Welded Super Duplex Stainless Steel

Yasser Reda[a], Aliaa Abdelfataah[b], Mohamed Abdel Azem[c], Hanan Abd El-Fattah[d*]

[a] *Chemical Engineering Department, Canal High Institute of Engineering and Technology, Suez, Egypt*

[b] *Mining, Petroleum and Metallurgical Engineering Department, Faculty of Engineering, Cairo University, Giza, Egypt*

[c] *Canadian International College, Egypt*

[d] *Department of Manufacturing Engineering and Production Technology, Modern Academy for Engineering and Technology, Egypt*

Abstract

Since stainless steel (SS) has many advantages such as excellent durability, ductility, and corrosion resistance. Duplex stainless steel (DSS) is a type of steel with superior resistance to localized and uniform corrosion. Mechanical properties of DSS with 26% chromium (Cr) were investigated under tensile, bend, impact, and hardness test. Chemical and Electrochemical corrosion tests were applied. The volume fraction of ferrite content in weld metal and heat effected zone was measured. Macro and microstructure examination were studied. DSS 26% Cr exhibited good mechanical properties and good corrosion resistance to pitting and uniform corrosion.

Keywords: Cr ASTM A790; microstructure; weight loss; mechanical properties; pitting corrosion.

1. Introduction

SS is a type of steel that contains a minimum percentage Cr of about 13%. The main characteristic specifies SS than other types is high corrosion resistance due to the presence of Cr which make a protective layer above steel. Excellent corrosion resistance of SS makes it a good candidate to use in corrosive medium and aquas environmental applications [1,2]. SS_S have many types some of them don't meet the main target of pitting corrosion resistance specially which used in sea water environment. Properties of every type of SS is dependent on the alloying elements added and its percentage [3]. DSS is a type of SS has superior properties than other types of SS. Alloying elements added to DSS are 20–28% Cr, 5% molybdenum (Mo), 9% nickel (Ni), and 0.05–0.5% nitrogen.

DSS consist of two phases ferrite α & austinite γ alloys that have combined properties of austenitic and ferritic stainless steels. The presence of austenite and ferrite phases with good percentages to each other in the microstructure would result in excellent and superior characteristics such as strength, toughness, and corrosion resistance [4]. As a result of welding of DSS the unbalanced microstructure appeared in zone of fusion moreover secondary phases were formed of. These significant transformations in microstructure have a direct effect on DSS welds characteristics.

DSS has an excellent cracking resistance behavior when used in sour environments due to the high percentage of Cr, Ni, Mo, and nitrogen. Many applications used DSS such as oil & gas transportation devices. These devices have a continuous exposure to hazardous chemicals so need a material with high resistance to corrosion and sulfide stress cracking [5]. Also, DSS is presently used in transporting petroleum products (liquids), and petroleum gases (CNG) [5]. Pitting potential range, pitting potentials, and conditions for the existence of pitting Corrosion considered as important factors that effect on pitting formation in stainless steels. The anodic metal dissolution process is dependent on potential. Moreover, this information is given by

*Corresponding author e-mail: hanan.abdelfattah@eng.modern-academy.edu.eg

Receive Date: 24 September 2023, Revise Date: 14 October 2023, Accept Date: 29 October 2023

DOI: 10.21608/ejchem.2023.238586.8658

analysis of the current-time relationship and the kinetics of pitting corrosion. Growth of pit occurred under different conditions such as galvanostatic, potentio-static, and chemical corrosion conditions. Pitting corrosion has different physical forms such as, pits shape which can be observed under different corrosion conditions and in different ranges of potential. The different corrosion conditions result in many shapes, for example hemispherical shaped pits, under-hollowing, elongated areal pits, and regular etch pits [6]. Active and passive states shouldn't multiply at same potential because the most pitting corrosion theoretical explanations belong to the principle of passivity. It discusses the circumstances in which stable pitting corrosion can occur. The effect of resistance polarization and concentration are discussed. The transference theory or transport and chemisorption process are discussed the pitting potentials and origin of pitting corrosion [7]. Pit generation induction time and pitting potential Statical variation have been investigated based on a theory of stochastic which was developed for the fracture occurred in solid materials due to different applied stresses [8]. Many data can be obtained by a different pitting corrosion testing device, which can measure the induction time and pitting potential for 12 specimens in 1 experiment by using 1 potentio stat. By made analysis of resulted data for type 304 SS in 3.5% NaCl solution, it is clear at constant potential the pitting process done by three successful processes. The potential sweep method is used for determining and detecting the pitting potential [9,10]. Pitting potential increases with the square root of the potential sweep velocity theory can be used in improving the prediction of experiment. Linear relation between pit generation rate and potential gives a suggestion that not only the electrochemical reaction is controlled the pitting process, but the electromechanical breakdown of the passive film can be considered as important factor [11-13]. In the presence of sodium sulfide weight loss investigations indicated that rates of corrosion in UNS44660 were lower than the other grades of SS. Linear polarization resistance and potentio-dynamic polarization measurements illustrated that the electrochemical behavior changed by sulfur species adhesion, due to reduction in polarization resistances and increasing in densities of anodic current. SEM and XPS results in mentioned references reveal to good conclusion that the surface films that made in caustic solution having sodium sulfide were imperfect because the adsorption of sulfide resulted destabilization in the formed passive film and formation of insoluble metal sulfide compounds [14-16].

In this work DSS 26% Cr mechanical properties were investigated. Macro and microstructure were studied before and after electrochemical corrosion test. All results were discussed to show the good mechanical properties and pitting corrosion resistance of DSS 26% Cr.

2. Experimental

2.1. Materials

Specimen of Cr ASTM A790 pipe is used in this investigation with thickness of about 2.5 mm, and length 25mm, with an immersed area around 1 cm2. Chemical composition investigated by Atomic Emission Spectrometer ARL3460 Advantage OES. Chemical composition is shown in table 1.

Table1: Chemical composition of Cr SS ASTM A790 pipe

B	C	N	Al	Si	P	S	Ca	Ti	V	Cr	Mn
0.0009	0.026	1.786	0.014	0.328	0.016	0.0009	0.0002	0.002	0.064	26.6	0.361
As	Zn	Nb	Mo	Sn	Sb	W	Pb	Bi	Fe	Cu	Ni
0.0007	0.004	0.007	3.54	0.007	0.009	0.561	0.004	0.037	57.125	0.41	8.72

2.2 Mechanical testing

Specimens are prepared using ASTM E8M and ASTM E23 for tensile, bend and Charpy tests respectively. SHIMADZU 100-ton universal testing machine was used for tensile and bend tests, while impact testing machine JB-W500 was used for impact test. Specimen of impact test dimensions were 10*10*55 mm. Notch was in the center of specimen with 45^{o}, 2 mm deep with 0.25 R, Striker Energy about 250 Joule. Also, a hardness test was applied by using Zwick/Rockwell ZHU250 hardness testing machine. About 33 points measured in the hardness test in different positions included base metal, welded metal and heat affected zone (HAZ). 2.3. Corrosion studies

2.2.1 Pitting corrosion test

The specimens were cleaned by using ethyl alcohol and then weigh by a highly sensitive Balance Sartorius te214s‹ before immersing in FeCl3 soln. prepared by adding 100gm of FeCl3 in 900ml DI water, then taking 600ml of soln. and diluted in 1000ml DI water. The test was conducted in water Bath at 400C for 24 hrs.

2.2.2. Studies of potentio-dynamic polarization

The electrochemical cell used a computerized PGZ potentio stat /Galvano stat VoltaLab6 was a standard three- electrode Pyrex glass cell at room temperature. A Calomel electrode was employed as the reference electrode, the counter electrode is fixed by using platinum foil. Cr ASTM A790 pipe specimens were used as a working electrode. A total area of the working electrode of about 1.0 cm2 was exposed to the 3.5% NaCl solution. The open-circuit potential (OCP) was registered for at least 30 min before each experiment. The studies of potentio-dynamic polarization were braced out in 3.5% NaCl solution. Polarization curves were reported after measurements of the electrochemical impedance, to test the outcome of the covering films under weathering efficiency of the alloy. polarization measurements were achieved at four different scan rates of (0.833, 2, 5, and 10) mVs^{-1} and at lab temperature indoors the range of potential from the cathodic to the anodic side (-0.5 to 0.5 V).

2.3. Surface examination

The superficial topography of Cr ASTM A790 pipe after corrosion in $FeCl_3$ is performed via JEOL JAX-840A electron micro-analyzer.

3. Results and discussion:

3.1 Mechanical tests

3.1.1 Tensile Test:

Two tubes were machined as tensile test specimens and conducted to the SHIMADZU 100-ton Universal Testing Machine in-order to test the base and weld materials. Table 2 shows the ultimate tensile strength (UTS) and the location of failure for the tested material. Table 2 shows the UTS ranges from 844-857MPa. Moreover, the failure location takes place at the base metal.

Table 2: The Ultimate Tensile strength and the Location of failure for the tested material

Test specimen	Measured Thickness, mm	Measured Width, mm	Effective Area, mm^2	Ultimate Tensile strength, MPa	Location of failure
Sample 1	21	19.2	403.2	844	B.M
Sample 2	20	20	400	857	B.M

Two another tensile specimens were conducted at the tensile machine for testing the welded area, the test was conducted in longitudinal axis of specimens. Table 3 shows the UTS and the yield stress for the welded tested material. Table 3 shows that the UTS ranges from 958-990 MPa, and the yield stress ranges from 905-916 MPa. The measured values are considered high as it compared with standard values [S32760] according to ASTM A790/A 790M-05 a [17].

Table 3: material The Ultimate Tensile strength and the Yield Stress for the welded tested

Test specimen	Measured diameter, mm	Yield Stress, MPa (0.5%)	Ultimate Tensile strength, MPa	Elongation %
Sample 1	12.5	916	990	28
Sample 2	12.4	905	958	29

3.1.2 Bend Test Result:

Four tubes were conducted at UH-1000KNX Universal Testing Machine for testing the defect appear due to bending under mandrel of diameter 40mm and under bending angle 180 deg. Table 4 shows the criteria of bend tested material. Table 4 shows that after the bend test, there is no appearance of any defect at the surface of the tested tubes.

Table 4: The criteria of bend tested materials.

Test Specimen	**Type of Bend Mandrel Diameter (Former) 40 mm**	**Bend Angle**	**Result**
1	SIDE	180 deg.	(No defects noted)
2	SIDE	180 deg.	(No defects noted)
3	SIDE	180 deg.	(No defects noted)
4	SIDE	180 deg.	(No defects noted)

3.1.3 Impact test

6 notched specimens (4 in cap and 2 root) were prepared for conducting impact testing machine JB-W500 250 Joule. The specimens were machined in dimensions (mm): 10.0*10.0*55.0 mm with V-notch, in the center of specimen with 45^{o}, 2 mm deep with 0.25 R using striker energy: 250 Joule, the test was conducted at - 46 ^{o}C. Table 5 shows the energy of tested material. Table 5 shows that the energy of welded metal in cap tested material is 113.3 J, while at cap, it ranges from 126.7-166.7 J. It also shows that in root the energy of welded metal is 100 J, while at root, it is 145J.It is concluded that the energy at cap is greater than that at root.

Table 5: The energy of tested material

Type of Specimen(s)/notch Location	CVN IN CAP				
	1st Value	2nd Value	3rd Value	Average	Test Side
WM - CAP	50	160	130	113.3	WELD METAL
F. L	185	65	130	126.7	CAP
F.L + 2	185	150	165	166.7	
F.L + 5	125	185	108	139.3	
Type of Specimen(s)/notch Location	CVN IN ROOT				
	1st Value	2nd Value	3rd Value	Average	Test Side
WM – 1	95	110	95	100.0	WELD METAL
F. L	60	250	125	145.0	ROOT

3.1.4 Hardness Test:

Specimens were tested by Zwick/Roell ZHU250 hardness testing machine in all the Base, weld metal and HAZ for about 33 points of measurements. Figure 1 shows the schematic drawing representing the measured specimen. Two specimens were tested in two directions at 3 O'clock and at 6 O'clock. As shown in Table 6, 7. From previous data, all measured points gives high hardness value as it compared with standard values [S32760] according to ASTM A790/A 790M-05 a. [17]

Figure 1: The Hardness measurements for tested specimen

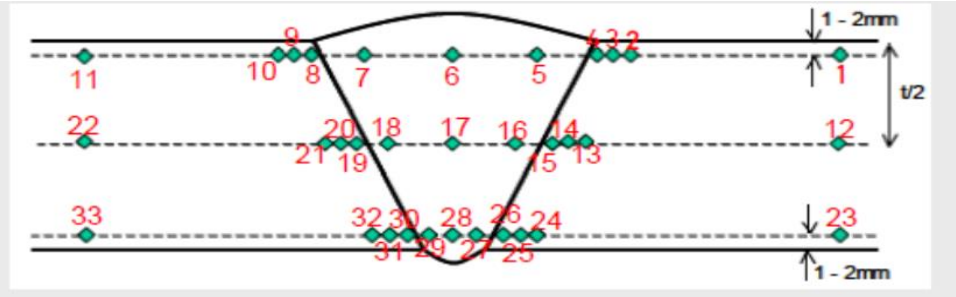

Table 6: The hardness values measured at 3 O'clock.

Sample1 (At 3 O'clock) HV 10										
BM SIDE A	HAZ SIDE A			WM			HAZ SIDE B			BM SIDE B
1	2	3	4	5	6	7	8	9	10	11
297	217	321	328	333	326	317	320	338	331	294
12	13	14	15	16	17	18	19	20	21	22
318	324	330	330	315	339	334	321	342	320	280
23	24	25	26	27	28	29	30	31	32	33
323	321	310	322	330	335	322	324	318	315	284

Table 7: The hardness values measured at 6 O'clock.

Sample2 (At 6 O'clock) HV 10										
BM SIDE A	HAZ SIDE A			WM			HAZ SIDE B			BM SIDE B
1	2	3	4	5	6	7	8	9	10	11
286	308	321	315	309	313	313	300	310	318	310
12	13	14	15	16	17	18	19	20	21	22
280	320	330	315	332	333	340	305	319	308	310
23	24	25	26	27	28	29	30	31	32	33
300	305	300	318	320	327	324	309	302	295	300

3.1.5 Ferrite Content:

Table 8 shows the ferrite content for four positions of welding (WM, HAZ) cap and root. These results show that ferrite content in HAZ region is higher than in cap region. Weld metal ferrite content is the main factor in which yield strength and resistance to chloride stress corrosion cracking (CSCC) are depending on. The required percentage should be from 30 to 60%, or 30 to 70 ferrite number [17]. As shown in table 8 ferrite content in different positions (cap, root, and HAZ) varying between 35 to 55.8% ferrite content. The percentage of ferrite boosts the good tensile strength results, and the corrosion resistance as will discussed later.

Table 8: the ferrite content for four position of weld (WM, HAZ) cap and root

Ferrite Content					
Serial No.	**Position**	**1st %**	**2nd%**	**3rd%**	**Volume fraction Vv(%)**
1	WM CAP	35.80	36.00	41.10	37.63
2	WM ROOT	45.50	45.50	44.50	45.17
3	HAZ CAP Area	53.50	54.90	51.40	53.27
4	HAZ ROOT Area	53.40	55.20	55.80	54.80

3.2. Corrosion test:

3.2.1 Pitting test

The tested specimens were polished to a 120-grit finish arid rinsed on an ultrasonic cleaner to remove any debris and then examined at a magnification X20 by stereomicroscope. The solution and bath water temperature should reach the identical temperature 40 ^{o}C, before the test specimen is placed in a one-liter beaker and maintained at 40 ^{o}C for 24 hours. After the 24-hour test period, the specimen was rinsed and cleaned in an ultrasonic cleaner to remove any debris, dried, weighted and evaluated. The specimen was then examined at X 20 magnification by Stereomicroscope. The specimen was weighed before the test and the initial weight was 202.0539g and at the end of the test the final weight was 202.0256g. The difference between the initial and the final weight is the weight loss. It was ٠.٠٢٨3g and the total subjected surface area was 69.42 cm^2. It was concluded the total corrosion rate was about 4.08 g/m^2. No visible pits on the surface of the sample at 20X magnification.

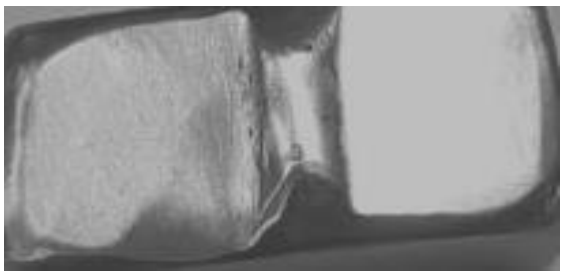

Before the test

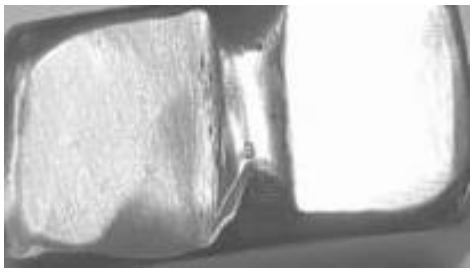

After the test

Figure 2: Images for DSS before and after pitting test

3.2 Electrochemical test

The electrochemical potentio-dynamic polarization curves of Duplex 26% Cr samples immersed in the 3.5% NaCl at different scan rates are presented in Figure 3. The corrosion resistance decreased with increasing scan rate. The corrosion rate is always found higher at high scan rate because of more discharge current on the surface and that can be observed by experiments [10].

3.3 Macro-Microstructure:

3.3.1 Macrostructure

The specimens were prepared with macrographic etchant soln. of Nitric Acid + Ethyl Alcohol in-order to prepare the surface. Location of picture is perpendicular to weld axis with magnification 5 X in two directions 3 and 6 O'clock. The Macrostructure shows no defects noted.

Figure3: Potentio-dynamic curves for DSS 26% Cr at different scanning rates

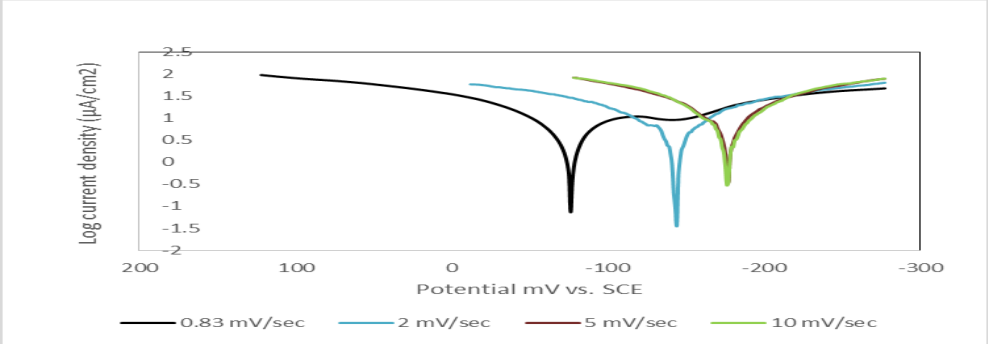

Figure 4: Macrographic of weld DSS in two direction 3 and 6 o`clock at 5 X

	
Macrostructure at 3 O'clock"	Macrostructure at 6 O'clock"

3.3.2 Microstructure Examination:

The specimens were prepared with micrographic etchant (20 % NaOH) 20 g NaOH, 100 ml H_2O in-order to prepare the surface with magnification 500 X in weld metal and HAZ in the cap and root area.

Figure 5 reveals the optical microstructure of the DSS 26% Cr. No obvious intermetallic compounds were observed in the grains or on the boundaries. Also, the microstructures show absence of carbides and nitrides [11]. DSS that has mixed phases and microstructure of austenite and ferrite, own better corrosion resistance and superior mechanical properties than austenitic SS [18].

The microstructure of DSS consists of 50% ferrite α and 50% austenite γ. These two-phases enhanced the DSS mechanical properties and corrosion resistance. The resulting microstructure is mainly dependent on the applied heat treatment and chemical composition. The temperature increases during welding processes in HAZ till retransformation of austenite into ferrite range, but due to high cooling rates aa part of ferrite only retransformed. Most of the standards limit of DSS the ferrite content in the range from 30 to 70% is important to achieve the good corrosion and mechanical properties which is achieved in this work [19]. The specimens exhibited good corrosion and pitting resistance. Also, exhibited good mechanical properties such as tensile test, hardness test and impact test.

4. Conclusion

Duplex stainless steel (DSS) is a type of steel with superior resistance to localized and uniform corrosion. Mechanical properties of DSS with 26% chromium (Cr) were tested under tensile, bend, impact, and hardness test. Chemical and Electrochemical corrosion tests were applied. Macrostructure examination was investigated perpendicular to the weld axis with no defects noted. Also, microstructure examination indicated the absence of intermetallic phases, carbides, and nitrides. It was concluded that the good mechanical properties of DSS 26% Cr accompanied good corrosion resistance to pitting and general corrosion.

Figure 5: Micrographic of DSS for different regions at 500 X, a: WM (cap), b: WM (root), C: HAZ (cap), D: HAZ (root).

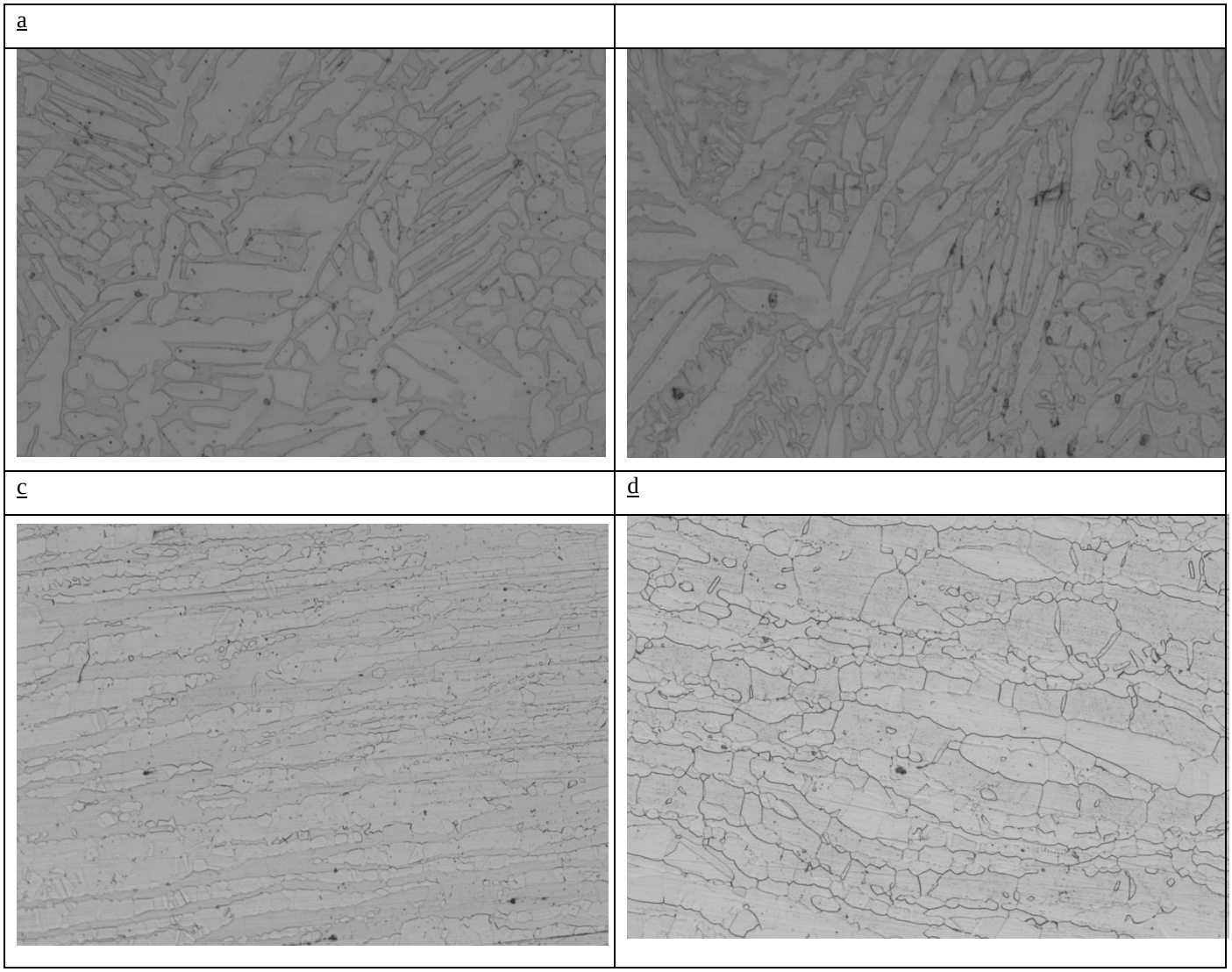

5. Conflict of interest

The authors declare that they have no conflicts of interest.

.**6. Acknowledgments**

The authors thank mechanical lab in Cairo university faculty of engineering.

7. References:

1- . Kim, S. K. Hong, B. Hwang, J. Kim. Block shear capacity in cold-formed lean duplex stainless steel double-shear bolted connections. Thin-Walled Structures. 161 (2021) 107520

2 -W. Schwenk. Theory of stainless-steel pitting. Corrosion. 4 (1964) 20

3 - M. M. Pariona. Correlation between microstructural and corrosion resistance of boron-modified duplex stainless-steel proceed by spray-forming. International Journal of Research. GRANTHAALAYAH. 9(5) (2021) 327

4 -L. Sharma, K. Sharma. Dissimilar welding of super duplex stainless steel (SDSS) and pipeline steel A brief overview. materials today proceeding. 2022

5 -R. Sivasubramani, V. Aarya, G. Rithvik, C. Utkarsh, S. Kumaran. Influence on nonhomogeneous microstructure formation and its role on tensile and fatigue performance of duplex stainless steel by a solid-state welding process. Material today proceeding. 46 (17) (2021) 7284-7296

6-Y.Tang, N. Dai, J. Wu, Y. Jiang, and J. Li. Effect of Surface Roughness on Pitting Corrosion of 2205 Duplex Stainless Steel Investigated by Electrochemical Noise Measurements. Materials (Basel). 12(5) (2019) 738

7 -T. Shibata, T. Takeyama. Stochastic Theory of Pitting Corrosion. Corrosion. 33 (7) (1977) 243–251

8 -N. Sridhar, R. Thodla, F. Gui, L. Cao and A. Anderko. Corrosion-resistant alloy testing and selection for oil and gas production, The International Journal of Corrosion Processes and Corrosion Control. 17th Asian Pacific Corrosion Control Conference. 1 (2018) 53

9-A. Kocijan, R. Donik, M. Jenko. The electrochemical study of duplex stainless-steel in chloride solutions. Materials and technology. 43(1) (2009) 39–42

10 -J. Zhang, X. Hu, P. Lin, and K. Chou. Electrochemical Behavior of 2205 Duplex Stainless Steel in a Chloride-Thiosulfate Environment. Int. J. Electrochem. Sci. 14 (2019) 4144 – 4160

11-K. R. Chasse & P. M. Singh. Corrosion Study of Super Ferritic Stainless Steel UNS S44660 (26Cr-3Ni-3Mo) and Several Other Stainless-Steel Grades (UNS S31603, S32101, and S32205) in Caustic Solution Containing Sodium Sulfide. Metallurgical and Materials Transactions A. 44 (2013) 5039–5053

12 -N. Kumar, M. K. Manoj, and M. K. Phani, Influence of Potential Scan Rate on Corrosion Behaviour of Heat-treated AA 7075 Alloy in Sulphuric Acid Solution. Material Science Research India. 15 (1) (2018) 91-99.

13 -J. Zhao, C. Yang, D. Zhang, Y. Zhao, M. S. Khan, D. Xu, T. Xi, X. Li and K. Yang. Investigation on mechanical, corrosion resistance and antibacterial properties of Cu-bearing 2205 duplex stainless steel by solution treatment. RSC Adv. 6 (2016) 112738

14-A. Marcos, S. Leite, M. Teradab, V. F. Pereira, E. B. da Fonseca, N. B. de Lima, I. Costa. On the pitting resistance of friction stir welded UNS S82441 lean duplex stainless steel. Journal of material and technology. 8(3) (2019) 3223–3233

15 -L. Esteves, M.M.A.M. Schvartzman, W. R. da Costa Campos, and V. F. C. Lins. Corrosion Behavior of Duplex Stainless Steel in Industrial White Liquor. Corrosion 74 (5) (2018) 543–550

16 -H. M. Ezuber. Corrosion Behavior of Heat-Treated Duplex Stainless Steels in Saturated Carbon Dioxide-Chloride Solutions. Journal of ASTM International. Paper ID JAI12866. 2 (2005) 5

17 -P. K. Nanavati, D. J. Kotecki, Sanjay N. Soman, Effect of weld metal ferrite content on mechanical properties and stress corrosion cracking resistance in 22 Cr 5 Ni duplex stainless steel. Welding in the World. 63 (2019) 793–805

18 -S. Li, Y. Wang, X. Wang. Effects of ferrite content on the mechanical properties of thermal aged duplex stainless steels. Materials Science & Engineering A. (2014) S0921-5093

19- A. Higelin, S. Le Manchet, G. Passot, S. Cissé, J. Grocki. Heat‑affected zone ferrite content control of a duplex stainless-steel grade to enhance weldability. Welding in the World. 66 (2022) 1503–1519